Analysis and design of a high gain non-isolated zero current switching bidirectional DC–DC converter for electric vehicles

Veera Venkata Subrahmanya Kumar Bhajana, Pavel Drabek & Rajesh Thumma

Published online: 15 Feb 2019.

Submit your article to this journal ☑

Article views: 688

View related articles ☑

View Crossmark data ☑

Taylor & Francis
Taylor & Francis Group

Analysis and design of a high gain non-isolated zero current switching bidirectional DC–DC converter for electric vehicles

Veera Venkata Subrahmanya Kumar Bhajana [a], Pavel Drabek[a] and Rajesh Thumma [b]

[a]Regional Innovation Centre for Electrical Engineering, University of West Bohemia, Pilsen, Czech Republic; [b]Department of Electronics and Communication Engineering, Anurag Group of Institutions, Hyderabad, India

ABSTRACT

This paper presents a dual inductor based current-fed bidirectional non-isolated DC–DC converter for energy storage applications. The main idea of this converter is to achieve a higher voltage conversion ratio by obtaining the operation of zero current switching. The proposed soft-switching bidirectional DC–DC converter reduces the turn-off switching losses with the aid of auxiliary network, where, the auxiliary network comprised with the resonant inductor and the resonant capacitor. This converter operates under two different operating modes such as a boost (discharge) and buck (charge) modes. In both the modes of converter operations, the IGBTs are operating under zero current turn-off in order to minimize the switch turn-off losses and to improve the efficiency of the converter. The principle of the operations and its theoretical analysis are validated by the experimental results using a 300W (50 V/250 V) converter system.

1. Introduction

In recent years, there is a lot of demand for power converter technology in energy back-up systems such as fuel cells and super capacitors. The isolated BDC's play significant role in battery backup systems to transfer the power in two directions as low voltage to high voltage and vice-versa. To achieve the high voltage gain upto 3 kV, a transformerless DC–DC converter [1] implemented with the help of cascade connection of switches and capacitor (Total 19 arrays), which is operated under hard-switching since the source voltage is 67.5–350 V. To achieve the high gain, there are different approaches followed by many researchers, among them, one is using voltage multipliers based on diode-capacitor [2–4]. High voltage gain converters were implemented with the inverse dual converter [5] which transfers the power flow in dual directions. These converters are used in SCRs as semiconductor devices to transfer the output power. In recent years, there have been a research on high voltage gain isolated fullbridge DC–DC converter [6] with high efficiency for battery storage applications. There are many current-fed isolated converters including push–pull [7] and half bridge [8] implemented as hard-switching version. Later on, the current-fed isolated converters (Boost) were developed to obtain the zero voltage switching (ZVS) [9] with the usage of snubber capacitors, transformer leakage inductances and current-fed high voltage gain resonant full bridge converters [10,11] with the help of

resonant capacitor connected parallel with an inductor. The different variations of current-fed isolated half-bridge converters with the usage of passive lossless and active lossless snubbers were reported [12–14] in order to obtain ZVS operations to their semiconductor switches. At the later stage of the ZVS in current-fed isolated converters research, many researchers worked to investigate the turn-off operation at zero current of IGBTs in the boost converter [15,16] and also soft-switching operation achieved in a resonant inverter [17] with the use of a parallel resonant tank. The isolated converters were developed with active clamp circuits [18–20] and the ZCS turn-off and ZVS turn-on [21,22] operations were achieved in this topology. A hard-switching multiphase high gain, high power non-isolated step-up converters [23] were compared and they reduced the input current ripple by the increased number of phases. Later, research was focused on non-isolated converters for the applications in battery backup systems to achieve the desired voltage levels, cost of design and reduction of size. A high voltage gain non-isolated boost converters [24] were implemented with an auxiliary passive resonant circuit in order to obtain soft-switching operations to their switching devices and diodes by means of the keeping resonant frequency below the switching frequency. Also, the researchers focused on secondary power supply systems in electric vehicles, and hence the work was concentrated on non-isolated BDC's [25] with the aid

CONTACT Veera Venkata Subrahmanya Kumar Bhajana ✉ bvvs.kumarfet@kiit.ac.in, kumarbvvs@yahoo.co.in, kumarbvv@rice.zcu.cz School of Electronics Engineering, KIIT University, Bhubaneswar-751024, Odisha, India

of simple series resonant elements which are used to obtain ZVS turn-on to their main switching devices. A non-isolated high gain boost converters [26] were developed with a parallel resonant circuit (LCC) and also an additional voltage multipliers cell. The zero voltage turn-on operation was achieved for main switches and Zero Current turn-on/off for diodes, respectively. However, lesser efficiency was obtained at very low power and high switching frequency (150 kHz). Similarly, a current-fed non-isolated bidirectional converter [27] was developed without voltage multiplier cells based parallel resonant circuit (LCL), it achieved the zero current turn-off operations of their switches and achieved 95.5% efficiency at the operating frequency above 100 kHz. There have been various non-isolated type converter topologies implemented under soft-switching condition. A passive lossless bidirectional converter [28] was operated with ZVS for the applications of electromechanical braking systems in electric vehicles. It is operated at very low input voltage, low power and low switching frequency. Nevertheless, it has obtained a maximum efficiency about 94% for very low output power conditions.

Based on previous existing high gain BDCs, both hard and soft-switching versions are considered in design to achieve the following issues: reduced switching losses, high power, high switching frequency and improved efficiency. A new non-isolated BDC has been proposed and implemented under zero current switching (ZCS) commutations. This article proposes a high gain non-isolated bidirectional DC–DC converter with the aid of additional active and passive resonant circuits. The main objective of the present research is to achieve the soft-switching operations to their respective switches with reduced switching losses.

2. Converter operation

The overall structure of the battery energy storage system of DC traction vehicles and the configuration of the proposed converter are shown in Figures 1 and 2, respectively. The circuit is basically comprised of six IGBTs (S_{1-4}, S_{p-q}), input inductors (L_1, L_2), auxiliary
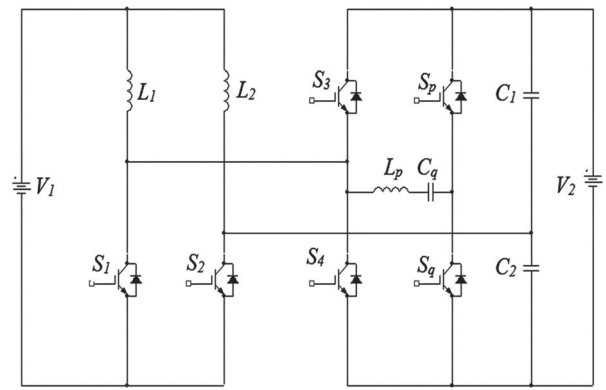

Figure 2. Proposed ZCS high gain bi-directional DC–DC converter.

inductor (L_p) and capacitor (C_q). When the converter is operated in boost mode, to transfer the power, the two IGBTs S_1,S_2 must be conducted and the additional IGBTs (S_p, S_q) is used to achieve soft-commutation of S_1, S_2. When this converter operates in buck mode, the output power is delivered by the IGBTs (S_2, S_3) by means of turning-on the auxiliary IGBTs (S_p, S_q), the turn-off of IGBTs S_2, S_3 occurs at zero current. The boost mode operation is explained based on the theoritcal waveforms as shown in Figure 3 and its equivalent circuits with the direction of current flow are shown in Figure 4.

2.1. Boost mode

First interval (t_0–t_1): At time t_0, the main IGBT S_1 is turned-on. The current flowing through the IGBT S_1 depends on the input inductor current. Prior to t_0, the IGBT S_2 is in conduction. Due to the resonance between L_p and C_q, the resonant tank current flows through the IGBT S_1. The current (i_{S1}) is expressed as;

$$i_{S1} = \frac{V_1}{L_P}(t_0 - t_1) - \frac{V_1}{Z}\cos(\omega(t_0 - t_1)) - I_o \quad (1)$$

The initial conditions of L_p and C_r are $i_{Lp}(0) = 0$; $V_{Cr}(0) = 0$, where, characteristics impedance $Z = \sqrt{\frac{L_p}{C_q}}$ and angular frequency $\omega = \frac{1}{\sqrt{L_p C_q}}$.
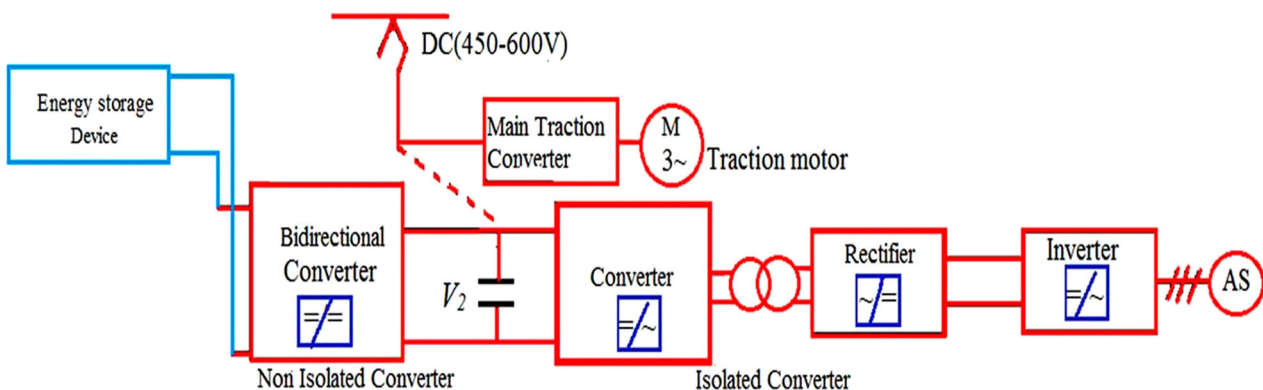

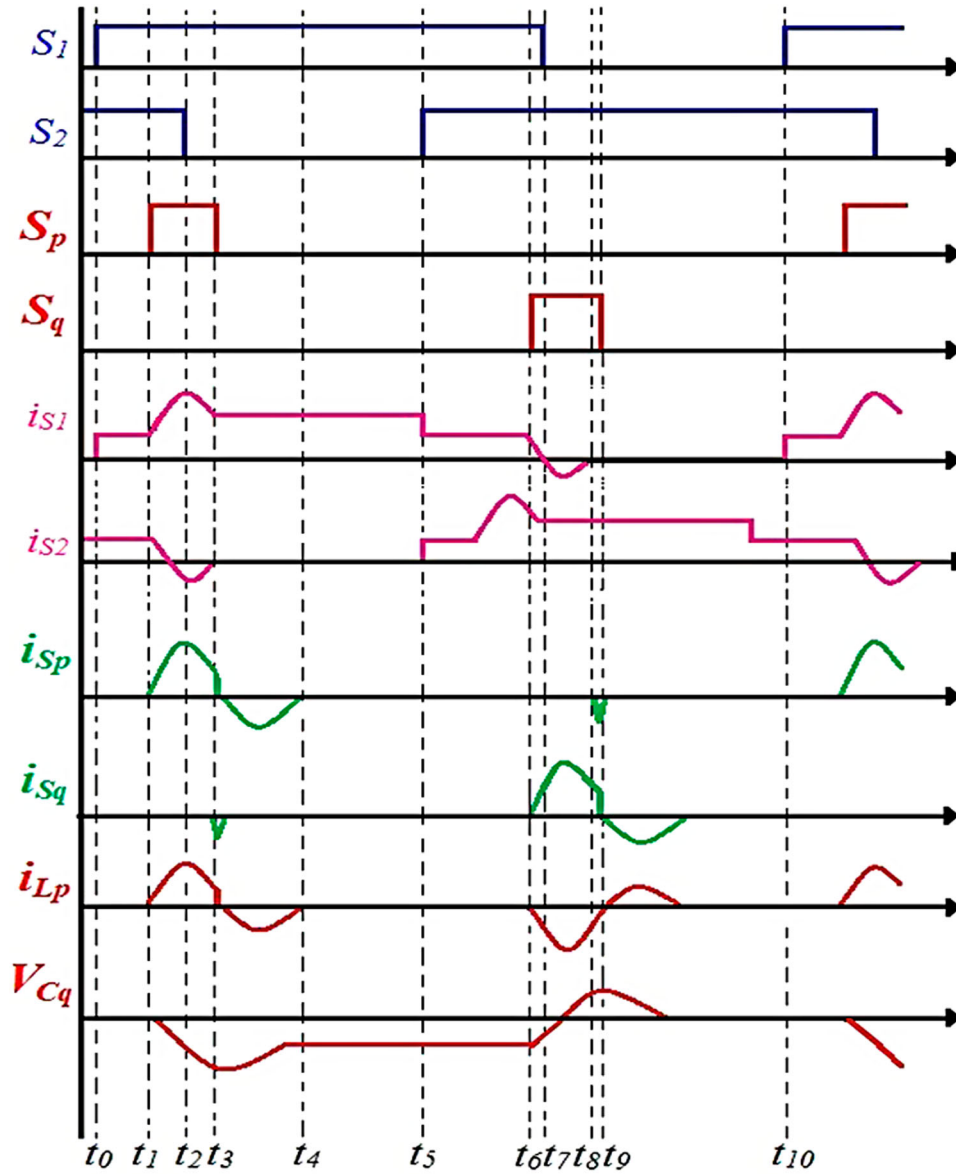**Figure 1.** Battery back-up systems in electric vehicles.

Figure 3. Theoretical waveforms: Boost mode.

Second Interval (t_1–t_2): At t_1, the auxiliary IGBT S_p is turned-on to achieve the ZCS turn-off of S_1 and S_2, then the current gradually reduces to zero. The energy is accumulating in the input inductor L_1 and the accumulated energy in L_2 is transferred as load at the instant of the IGBT S_2 turned-off. At t_2, the current of IGBT S_1 is identical to the output current I_o at t_2.

At t_2, the IGBT S_2 anti-parallel diode is still in conduction. The S_2, S_p currents and voltage of auxiliary capacitor C_q is expressed as;

$$i_{S2} = I_o - \frac{V_1}{Z}(t_1 - t_2)\cos\omega(t_1 - t_2) \quad (2)$$

$$i_{Sp} = -I_{in}\cos\omega(t_1 - t_2) - \frac{V_o - V_{Cq}}{Z}\sin\omega(t_1 - t_2) \quad (3)$$

$$V_{Cq} = -V_1\cos\omega(t_1 - t_2) \quad (4)$$

Third Interval (t_2–t_3): At t_2, the anti-parallel diode of IGBT S_2 is turned-on to allow the reverse current and

the anti-parallel diode of IGBT S_2 is turned-off at t_3. The current of S_2 is expressed as:

$$i_{S2} = I_o - I_o\cos\omega(t_2 - t_3) - \frac{V_{Cq} - V_o}{Z}\sin\omega(t_2 - t_3) \quad (5)$$

Fourth Interval (t_3–t_4): At time t_3, the IGBT S_2 is turned-off since the IGBT S_1 is turned-on from t_0 and a negative current flow through the IGBT S_p. Therefore, the anti-parallel diode of S_p is turned-on. The accumulated energy by the inductor L_2 is transferred to load via L_2-C_2-R. At the end of this interval, the anti-parallel diode of the IGBT S_p is turned-off.

Fifth Interval (t_4–t_5): During this interval, the IGBT S_1 remains in conduction and then the output power transfers via V_1–L_1–S_1.

Sixth Interval (t_5–t_6): This interval is similar to t_0–t_1; the IGBT S_1 remains in conduction except the applied gating signals to S_2.
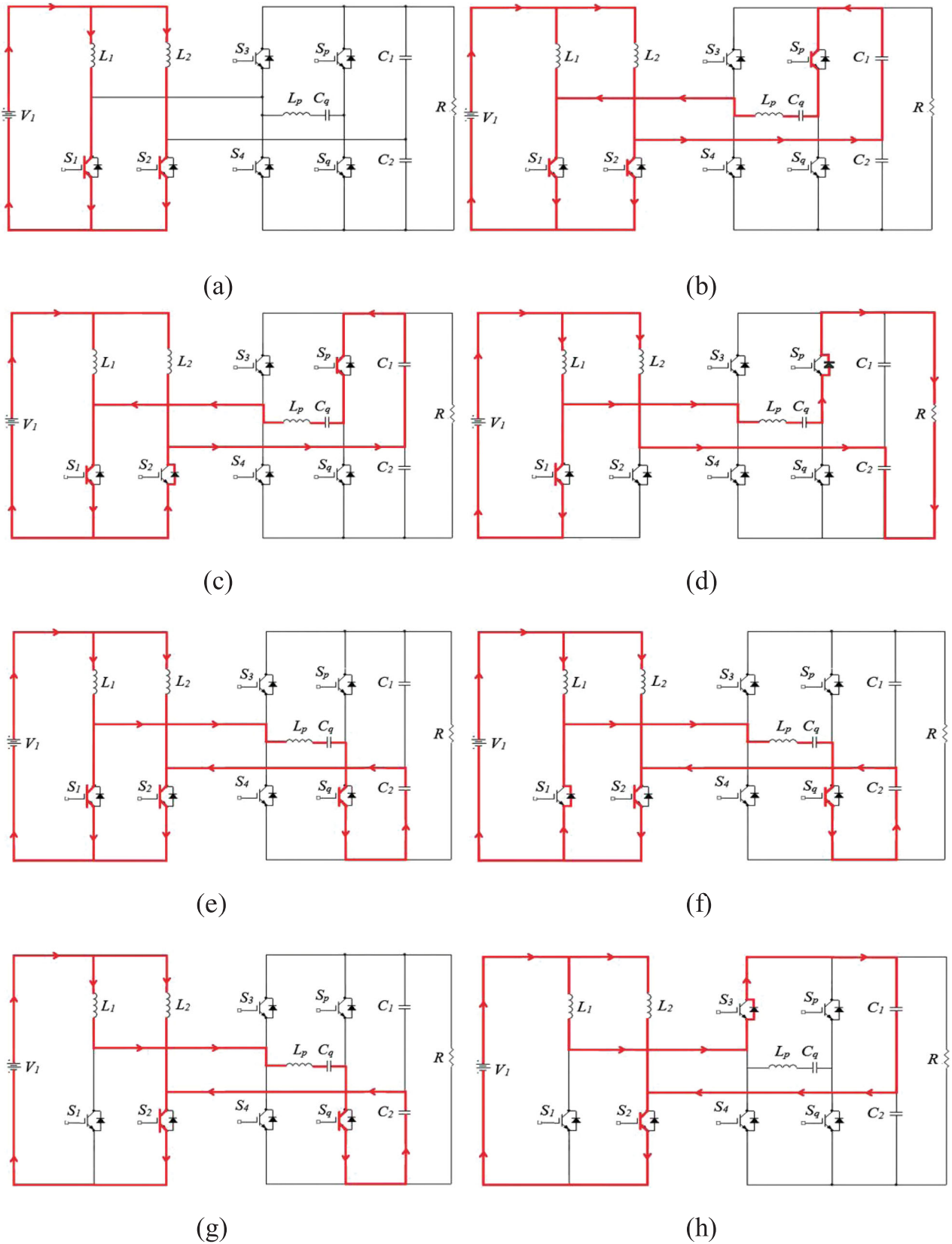
Figure 4. Current flow equivalent circuits of each interval -boost mode Interval (a) (t_0-t_1) & Interval (t_5-t_6) (b) Interval (t_1-t_2) (c) Interval (t_2-t_3) (d) Interval (t_3-t_4) (e) Interval (t_6-t_7) (f) Interval (t_7-t_8) (g) Interval (t_8-t_9) (h) Interval (t_9-t_{10}).

Seventh Interval (t_6-t_7): The auxiliary IGBT S_q is turned-on at t_6 to obtain the turn-off at zero current for S_2, while, the IGBT S_1 current gradually reduces to zero and then it becomes reversed. This time interval is called as the resonating interval. The resonant tank current produced by L_p,C_q is used to obtain the soft turn-off. The voltage and current expressions are defined as follows:

$$V_{Cq} = V_1 \cos \omega (t_6 - t_7) \qquad (6)$$

$$i_{Lp} = -\frac{V_{Cq}}{\sqrt{L_p/C_q}} \sin \omega(t_6 - t_7) \qquad (7)$$

Eighth Interval (t_7–t_8): At t_7, the anti-parallel diode of the IGBT S_1 is turned-on and resonant current flows through it. At t_8, the resonant tank current becomes zero and anti-parallel diode is turned-off. The voltage and current expressions of L_p, C_q are defined as follows:

$$V_{Cq} = V_o \cos \omega(t_7 - t_8) + I_i L_p \omega \sin \omega(t_7 - t_8) \quad (8)$$

$$i_{Lp} = I_i \cos \omega(t_7 - t_8) - \frac{V_{Cq}}{\omega L_p} \sin \omega(t_7 - t_8) \qquad (9)$$

Ninth Interval (t_8–t_9) and *Tenth Interval* (t_9–t_{10}) are the same as the period from t_2–t_4.

2.2. Buck mode

The operation of this mode is discussed based on the theoretical waveforms as shown in Figure 5 with principal waveforms of buck mode. The IGBTs S_3, S_4 are the main switching devices used to transfer the power to the output. The duty cycles of both the IGBTs S_3 and S_4 are about 50%. During this entire mode, the IGBTs S_1, S_2 are turned-off, however, the anti-parallel diodes give the path to flow the output current. The buck operation is divided into nine intervals and their current flow equivalent circuits are illustrated in Figure 6 and explained as below.

First Interval (t_0–t_1): At time t_0, the IGBT S_3 is turned-on, there is a current peak through the IGBT S_3 due to
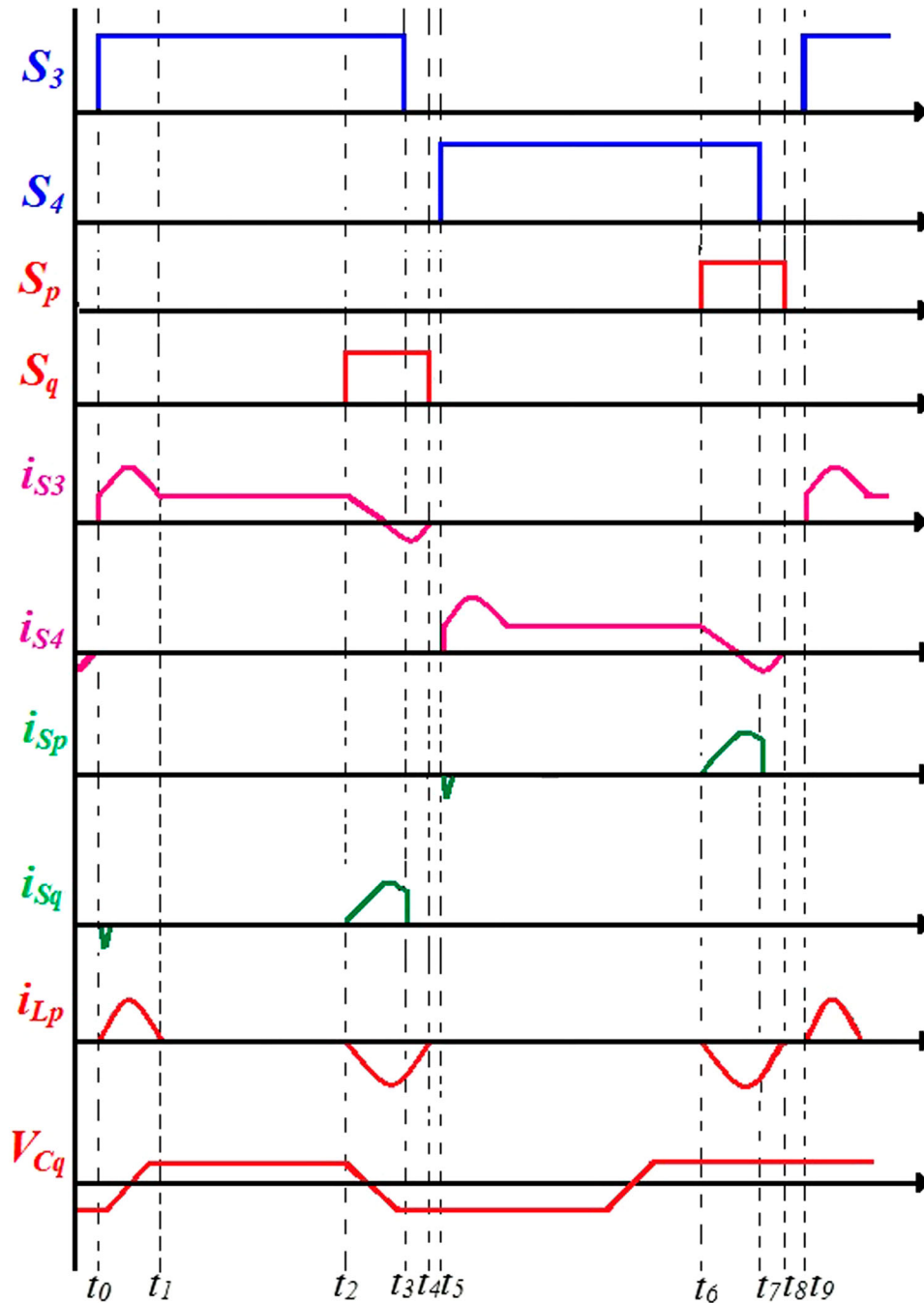

Figure 5. Theoritical waveforms: Buck mode. (a) Interval (t_0–t_1) & Interval (t_1–t_2) (b) Interval (t_2–t_3) (c) Interval (t_3–t_4) (d) Interval (t_4–t_5) (e) Interval (t_5–t_6) (f) Interval (t_6–t_7).
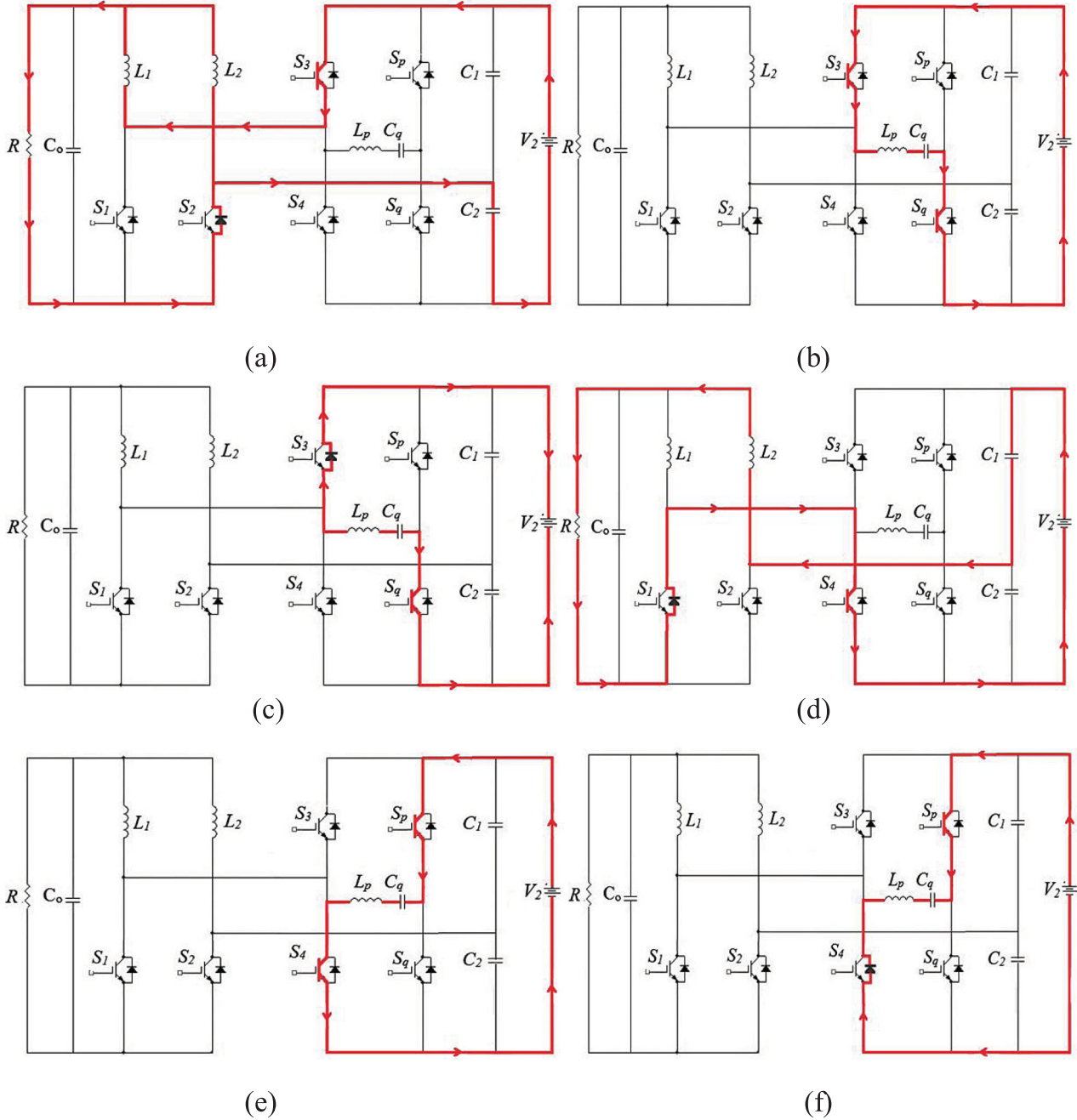
Figure 6. Current flow equivalent circuits of each interval-buck mode (a) Interval $(t_0 - t_1)$ & Interval $(t_1 - t_2)$, (b) Interval $(t_2 - t_3)$, (c) Interval $(t_3 - t_4)$, (d) Interval $(t_4 - t_5)$, (e)Interval $(t_5 - t_6)$, (f) Interval $(t_6 - t_7)$.

the resonant tank current produced by L_p, C_q. At the end, the current of the L_p becomes zero and voltage of C_q is charged to half of its input voltage.

Second Interval (t_1–t_2): For this whole interval, the output power transfers via the input capacitor C_1, input inductor L_1, anti-parallel diode of the IGBT S_2 and the main IGBT S_3.

Third Interval (t_2–t_3): At time t_2, the auxiliary IGBT S_q is turned-on to obtain the soft turn-off of the IGBT S_3. During this stage, the L_p, C_q are in resonating each other and IGBT S_3 current reduces gradually and it reaches zero at t_3.

Fourth Interval (t_3–t_4): During this interval, all IGBTs are in switched-off except the auxiliary IGBT S_q, so it is named as the switch-off period. In order to create a

path for resonance, the anti-parallel diode of S_3 starts conducting.

Fifth Interval (t_4–t_5): At this period of interval, all IGBTs are in switched-off for a while.

The Sixth (t_5–t_6), Seventh (t_6–t_7), Eighth (t_7–t_8) intervals are same as from t_0–t_1 to t_2–t_3 intervals, where the IGBT S_4 is operated and auxiliary IGBT S_p is used for obtaining zero current turn-off.

Ninth Interval (t_8–t_9): This interval is similar to the Fifth interval.

3. Design analysis

The proposed converter design analysis is described in this section. The design of auxiliary active circuit with
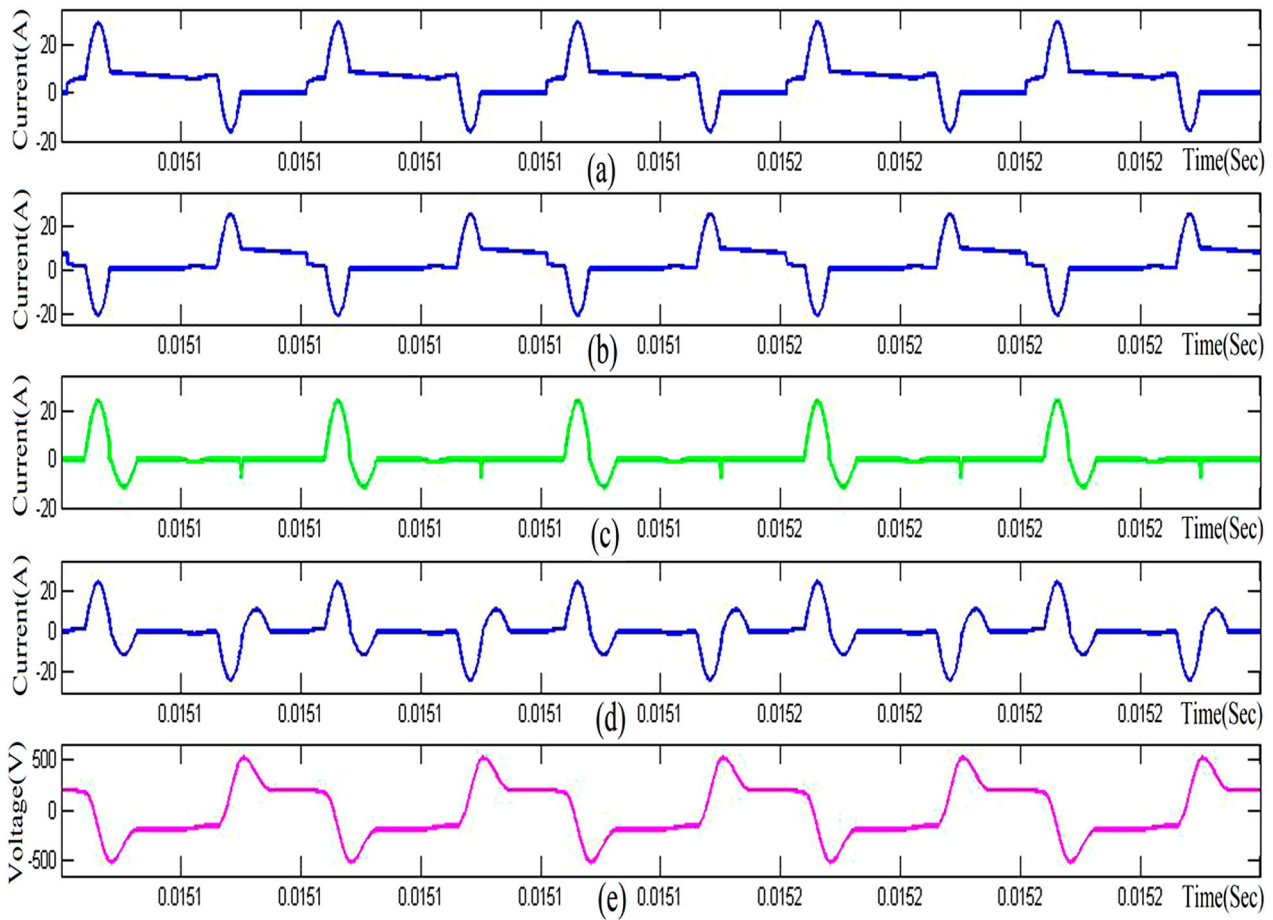
Figure 7. Simulation waveforms of boost mode opearation (a) I_{S1} - current through the switch current S_1, (b) I_{S2} - current through the switch current S_2, (c) I_{Sp} - current through the auxiliary switch current S_p, (d) I_{Lp} - current through the resonant inductor L_p, (e) V_{Cq} - voltage across the resonant capacitor boost mode.
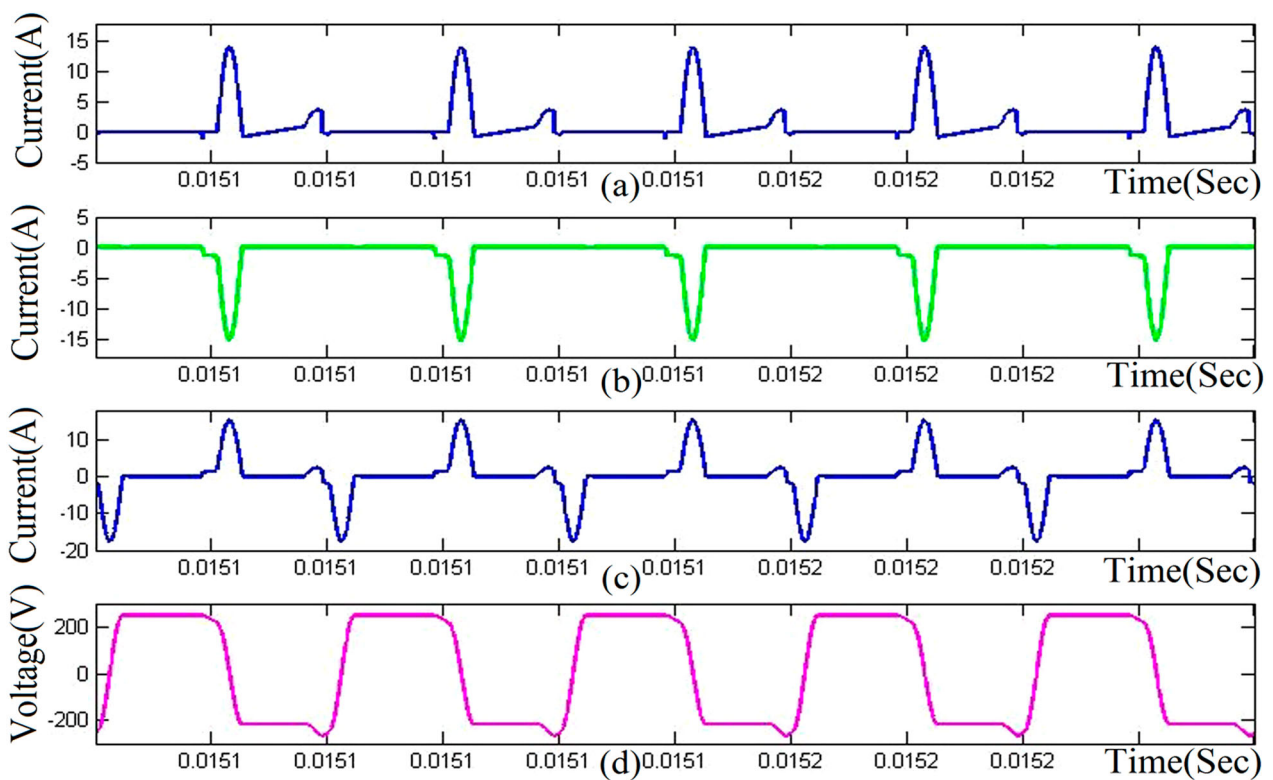

Figure 8. Simulation waveforms of buck mode operation (a) I_{S3} - current through the switch S_3, (b) I_{Sp} - current through the switch S_p, (c) I_{Lp} - current through the resonant inductor current of L_p, (d) V_{Cq} - voltage across the resonant capacitor.

a series resonant elements was considered to attain the zero current switching turn-off of the semiconductor switching devices, regardless of the direction of power transfer in this converter. There is an increase in current at turn-on of IGBTs S_{1-4} in both boost and buck modes due to the flow of resonant tank current. The

Table 1. Parameters considered for the proposed converter.

Parameter	Symbol	Value
Input voltage	V_1	50V
Output voltage	$V_o(V_2)$	250V
Maximum output power	P_o	300W
Switching frequency	f_{sw}	50kHz
Input inductor	L_{1-2}	200µH
Resonant inductors	L_p	20µH
Resonant capacitors	C_q	50nF
Output capacitor	C_o	470µF
Main switches	S_{1-4}	IKW40N120H3
Auxiliary switches	S_{p-q}	IKW40N120H3

values chosen for the resonant capacitor (C_q) is based on the values of the peak resonant tank current through the IGBTs(S_1-S_2). The higher values of the resonant capacitor (C_q) will reduce the peak current through the IGBTs S_1,S_2 and vice versa. The total period of resonance that is equal to the soft-turn-off period, it may increase or decrease depends on the values of resonant capacitor C_q. The larger value of L_p resonant inductance creates the zero current turn-off of the IGBTs (S_{1-4}).

The DC voltage conversion ratio can be determined by the analysis given by equation (10).

$$\frac{V_o}{V_{in}} = \frac{1}{2\pi}\frac{f}{f_r}\left(\frac{k}{2} + \frac{1}{k} - \sqrt{\frac{1}{k^2} - 1} + 2\pi - \sin^{-1}k\right)$$
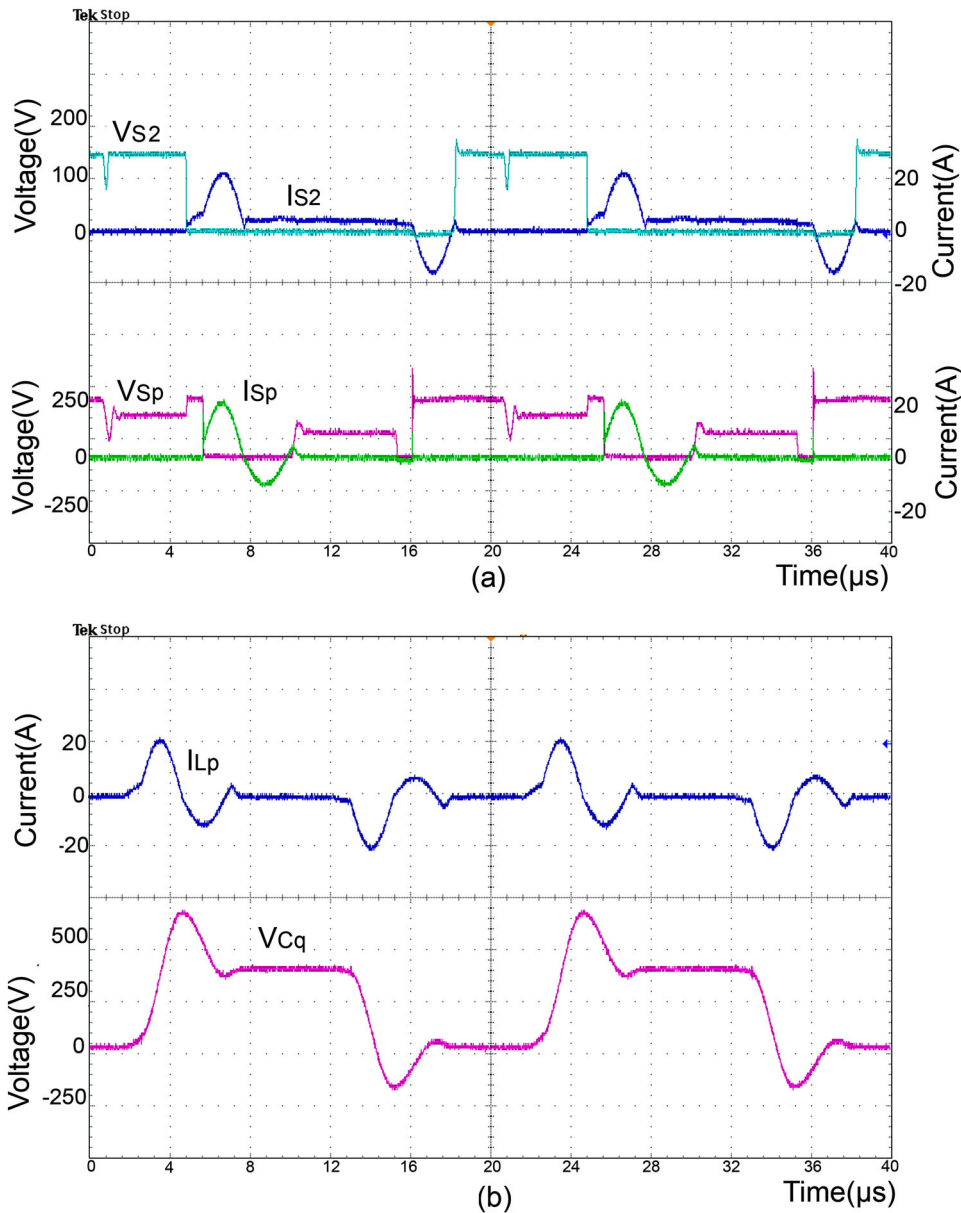$$+ \frac{\delta t}{T} \qquad (10)$$

Figure 9. Experminetal waveforms of boost mode opearation (a) switch S_2 collector current I_{S2} and the voltage across the collector to emitter V_{CE} & switch S_p collector current I_{Sp} and the voltage across the collector to emitter V_{CE} (b) Current through the inductor L_p and voltage across the capacitor C_q.

where V_o – Output voltage; V_{in} – Input voltage; k – Constant; f – Switching frequency; f_r – Resonant frequency; $\frac{\delta t}{T}$ – Duty cycle.

The behaviour of this converter is represented by a simplified Equation (11), $\frac{f}{f_r}$ is fixed value and the output voltage can be controlled by varying $\frac{\delta t}{T}$, The duration of from t_3–t_5 equals to δt, where $\delta t = t_5 - t_3$. The maximum value of $\frac{\delta t}{T}$ is given by Equation (12).

$$\frac{V_o}{V_{in}} = \frac{f}{f_r} + \frac{\delta t}{T} \quad (11)$$

$$\left(\frac{\delta t}{T}\right)_{max} = \frac{V_o}{V_{in}} - \frac{f}{f_r} \quad (12)$$

$$f_r = \frac{1}{2\pi\sqrt{L_P C_q}} \quad (13)$$

The ZCS turn-off condition for S_{1-4} can be obtained if Equation (14) is satisfied when the parameter (k) is less than one ($k < 1$).

$$k = \frac{I_m}{V_i}\sqrt{\frac{L_p}{C_q}} \leq 1 \quad (14)$$

where, maximum current of input inductor $I_m = \frac{P_m}{V_o}$, output voltage is V_o, the auxiliary inductance is L_p, and C_q is the auxiliary capacitance.

The parameters of resonant circuit can be defined as,

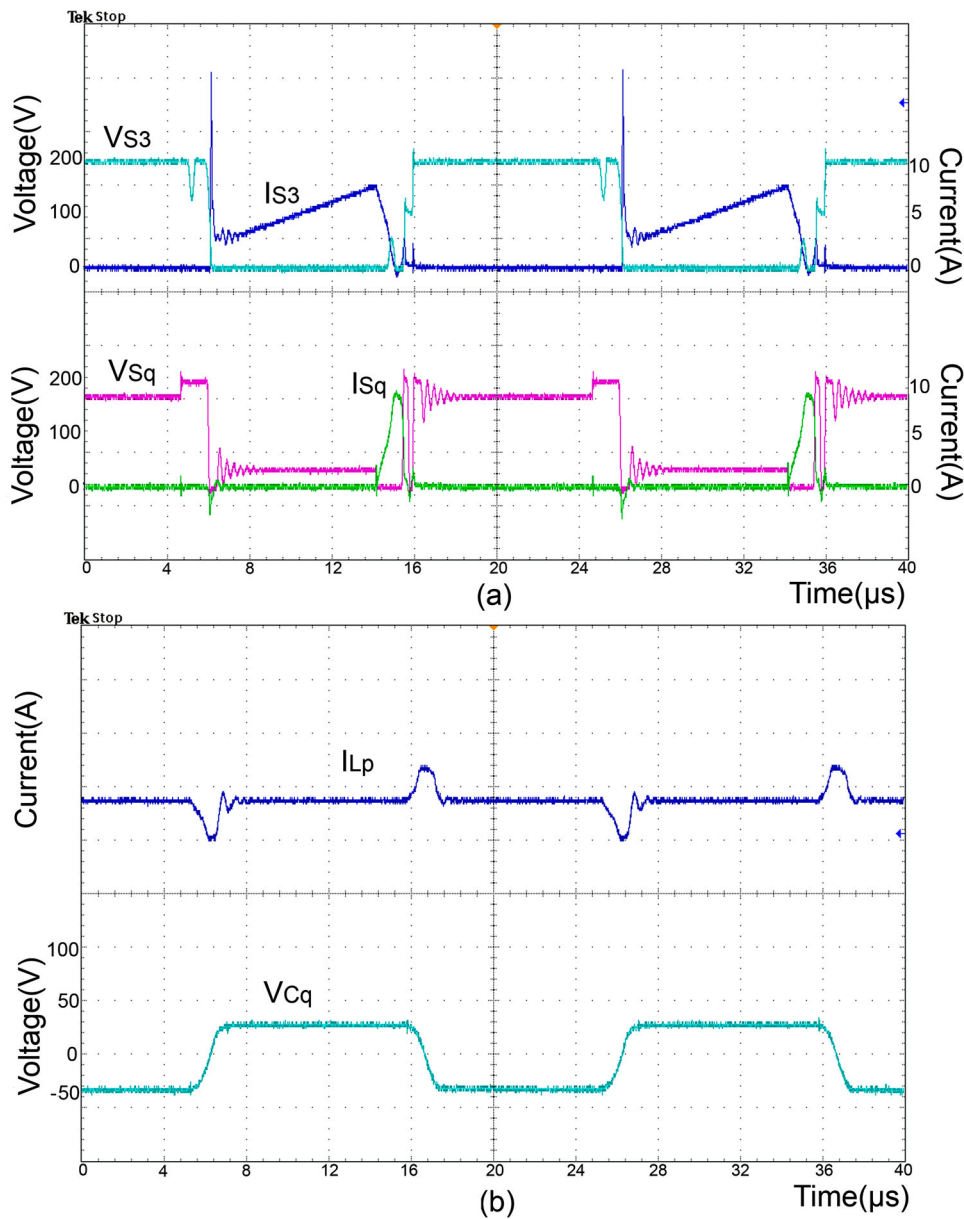$$\frac{L_p}{C_q} = \frac{1}{(2kf_r)^2} \quad (15)$$

Figure 10. Experminetal waveforms of buck mode opearation (a) switch S_3 collector current I_{S3} and the voltage across the collector to emitter V_{CE} & switch S_q collector current I_{Sq} and the voltage across the collector to emitter V_{CE} (b) auxiliary resonant inductor current I_{Lp} and auxiliary resonant capacitor voltage V_{Cp}.

3.1. Design example

The design is considered with the specifications of, 50 V input voltage; 250 V output voltage; 300 W output power and 50 kHz switching frequency.

The maximum input current $I_m = 1.2A$ (boost mode).

The maximum input current $I_m = 5.6A$ (buck mode).

The resonant frequency of auxiliary circuit is calculated as, $f_r = \frac{1}{2\pi \sqrt{L_p C_q}} = 0.159$ MHz.

The auxiliary inductor L_p and capacitor C_q values are chosen as, $L_p = 20 \,\mu H$; $C_q = 50 \,nF$. The ZCS turn-off condition is obtained at $k = 0.74$ and $k = 0.76$ from (15), which satisfies the condition $k < 1$.

4. Simulation and experimental evaulations

Initially, the soft-switching operations are observed by simulations, which are performed on MATLAB Simulink by considering the applied source voltage of 50 V in boost mode and 250 V in buck mode. The operating frequency of this converter is about 50 kHz and resonant circuit frequency of 0.159 MHz, which is obtained by equation (13). If equation (14) satisfies the condition, then the soft-switching can be obtained for their main IGBTs. This converter is designed and verified on open-loop simulation performance. The waveforms observed for the boost mode, the collector–emitter voltage (V_{CE}) and collector currents

(I_C) of the IGBTs (S_1, S_2), auxiliary inductor L_p current, auxiliary capacitor C_q voltages are depicted in Figure 7(a–d), which confirms the ZCS turn-off of the IGBT S_1 and auxiliary IGBTs S_p. Likewise, the simulations were performed for the buck mode and the observed waveforms are shown in Figure 8(a–d). To validate the simulation results of the converter design, a laboratory prototype was implemented for 50 V/250 V system by using the components and specifications as mentioned in Table 1. The duty cycles of 66% and 45% were used for the boost and buck modes, respectively. The Infineon IKW40N120H3 (IGBTs S_{1-4}, S_{p-q}) of six numbers were used in the prototype. The ferrite core E70 type auxiliary inductor with air gap of 3.5 mm was used to obtain a value of 20 μH inductance (three ferrite cores were used). Figure 9(a) shows the voltage V_{CE} and its current of the IGBTs S_1, S_q. From these measured waveforms, it confirms that the ZCS turn-off was obtained for the IGBT S_1 and soft turn-off of the auxiliary IGBT S_p.

Therefore, this converter has reduced switching losses. The measured waveforms of current of the auxiliary inductor L_p and voltage of auxiliary capacitor C_q are shown in Figure 9(b). Similarly, the experimental results were observed for buck mode. The voltage V_{CE}, currents of IGBTs S_3 and S_p are shown in Figure 10(a). Since the auxiliary resonant devices L_p and C_q are seriesly connected with the IGBT S_p, when it is turned-on, there is a voltage stress observed. However, the voltage of the IGBT is equal to 200 V
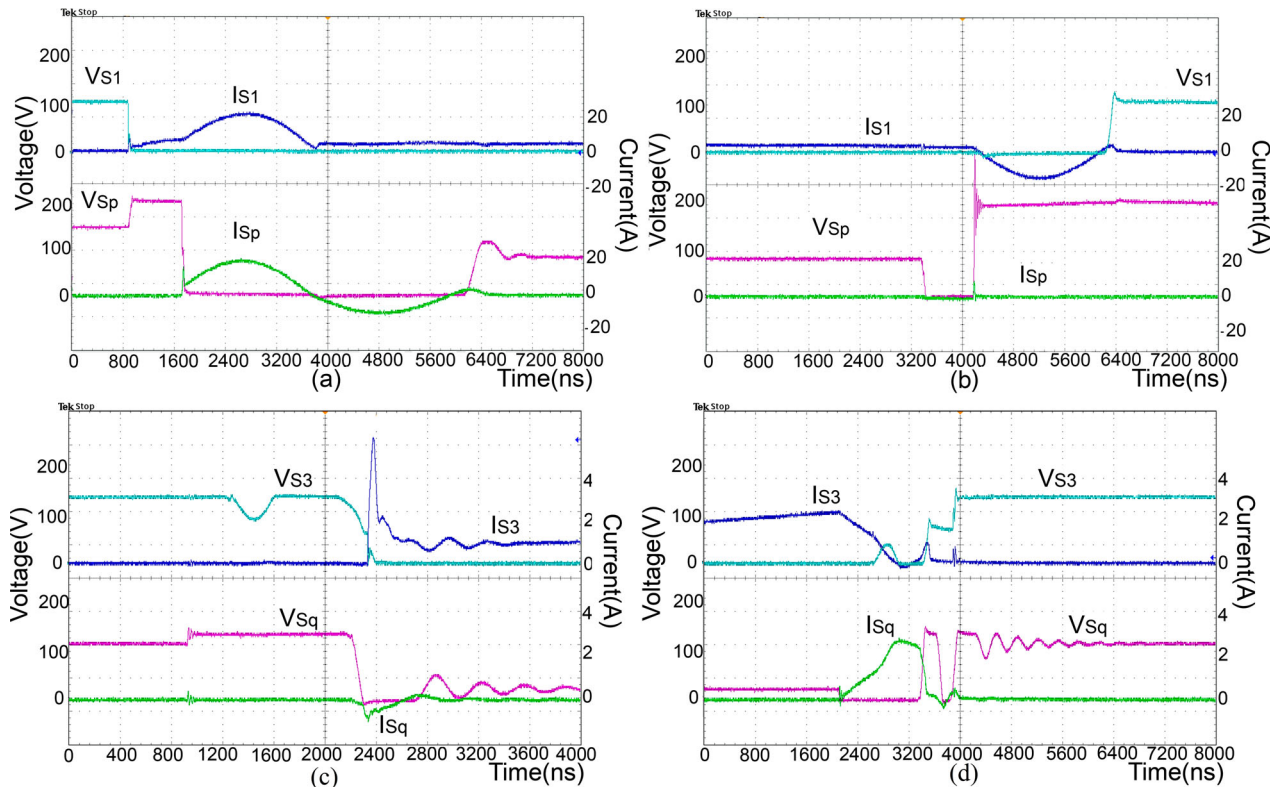

Figure 11. (a) Turn-on transition of IGBTs S_1 and S_p: boost mode. (b) Turn-off transition of IGBTs S_1 and S_p: boost mode. (c) Turn-on transition of IGBTs S_3 and S_p: buck mode. (d) Turn-off transition of the IGBTs S_3 and S_p: buck mode.
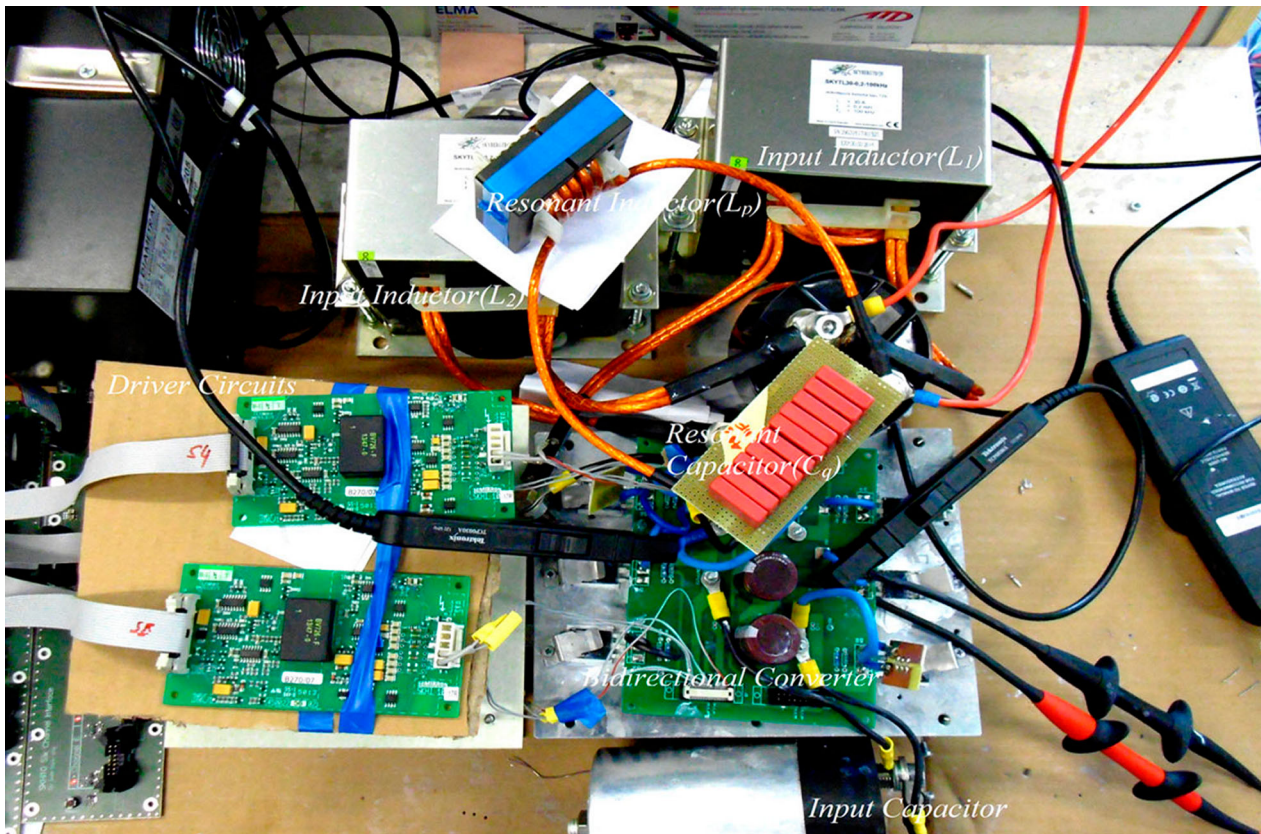
Figure 12. Experimental setup of proposed converter system.

when the input voltage of 300 V applied to the converter. The experimental waveforms of the auxiliary inductor L_p current and capacitor C_q voltage for buck mode are shown in Figure 10(a,b). Figure 11(a,b) shows turn-on/turn-off transition of the IGBT S_1 and auxiliary IGBT S_p at boost mode. Figure 11(c,d) depicted the turn-on and turn-off transitions for the IGBT S_3 and IGBTs S_p in buck mode. The experimental results were validated with the expected simulation analysis. The photograph of the experimental setup of this converter is shown in Figure 12.

5. Conclusion

A new soft-switching high gain bidirectional converter was designed and theoretically analysed. This converter was operated in forward power transfer (boost) and reverse power transfer (buck) modes with the aid of the auxiliary IGBTs, auxiliary inductor and capacitors. The main IGBTs are turn-off under ZCS is obtained, while converter operates in boost and buck modes. A laboratory prototype of 300 W and 50 V/250 V converter system was developed, tested and verified theoretically. This converter was tested at 300 W output power for both the operating modes. The soft-commutation ZCS was obtained for the IGBTs by way of the reduced turn-off switching losses. According to the efficiency analysis, the proposed topology achieved 95.5% and 96.84% for forward and reverse power transfer modes at 300 W

output power. The proposed converter was verified the soft-switching capability and it can be applied for higher power electric vehicles.

Disclosure statement

No potential conflict of interest was reported by the authors.

ORCID

Veera Venkata Subrahmanya Kumar Bhajana http://orcid.org/0000-0003-3830-7422
Rajesh Thumma http://orcid.org/0000-0003-4181-4572

References

[1] Sridharan G. Transformerless DC/DC converter for production of high voltage. Conference Record of the 1990 IEEE Industry Applications Society Annual Meeting; Seattle, WA; 1990, p. 1286–1288, Vol. 2.
[2] Franco LC, Pfitscher LL, Gules R. A new high static gain nonisolated DC–DC converter. Power Electronics Specialist Conference, 2003. PESC '03. 2003 IEEE 34th Annual; Acapulco, Mexico; 2003, p. 1367–1372, Vol. 3.
[3] Shenkman A, Berkovich Y, Axelrod B. The transformerless AC–DC and DC–DC converters with a diode-capacitor voltage multiplier. 2003 IEEE Bologna Power

Tech Conference Proceedings; Bologna, Italy; 2003, p. 6, Vol. 1.

[4] Ismail EH, Al-Saffar MA, Sabzali AJ. High conversion ratio DC–DC converters with reduced switch stress. IEEE Trans Circuits Syst Regul Pap. 2008;55(7):2139–2151.

[5] Ehsani M, Laskai L, Bilgic MO. Topological variations of the inverse dual converter for high power DC–DC applications. Conference Record of the 1990 IEEE Industry Applications Society Annual Meeting; Seattle, WA; 1990, p. 1262–1266, Vol. 2.

[6] Nymand M, Andersen MAE. A new approach to high efficiency in isolated boost converters for high-power low-voltage fuel cell applications. 2008 13th International Power Electronics and Motion Control Conference, Poznan; 2008, p. 127–131.

[7] Thottuvelil VJ, Wilson TG, Owen HA. Analysis and design of a push-pull current-fed converter. 1981 IEEE Power Electronics Specialists Conference; Boulder, CO; 1981, p. 192–203.

[8] Severus RP. A new current-fed converter topology. 1979 IEEE power Electronics Specialists Conference, San Diego, CA; 1979, p. 277–283.

[9] Han S-K, Yoon H-K, Moon G-W, et al. A new active clamping zero-voltage switching PWM current-fed half-bridge converter. IEEE Trans Power Electron. 2005;20(6):1271–1279.

[10] Steigerwald RL. High-frequency resonant transistor DC–DC converters. IEEE Trans Ind Electron. 1984;IE-31(2):181–191.

[11] Ivensky G, Gulko M, Ben-Yaakov S. Current-fed multi-resonant DC–DC converter. Proceedings Eighth Annual Applied Power Electronics Conference and Exposition, San Diego, CA; 1993, p. 58–64.

[12] Kim J-T, Lee B-K, Lee T-W, et al. An active clamping current-fed half-bridge converter for fuel-cell generation systems. 2004 IEEE 35th Annual Power Electronics Specialists Conference (IEEE Cat. No.04CH37551); 2004, p. 4709–4714, Vol.6.

[13] Jang SJ, Won CY, Lee BK, et al. Fuel cell generation system with a new active clamping current-fed half-bridge converter. IEEE Trans Energy Convers. 2007;22(2):332–340.

[14] Mohammadi M, Adib E. Lossless passive snubber for half bridge interleaved flyback converter. IET Power Electron. 2014;7(6):1475–1481.

[15] Chen JF, Chen RY, Liang TJ. Study and Implementation of a single-stage current-fed boost PFC converter with ZCS for high voltage applications. IEEE Trans Power Electron. 2008;23(1):379–386.

[16] Chen RY, Liang TJ, Chen JF, et al. Study and implementation of a current-fed full-bridge boost DC–DC converter with zero-current switching for high-voltage applications. IEEE Trans Ind Appl. 2008;44(4):1218–1226.

[17] Liang TJ, Chen RY, Chen JF. Current-fed parallel-resonant DC–AC inverter for cold-cathodefluorescent lamps with zero-current switching. IEEE Trans Power Electron. 2008;23(4):2206–2210.

[18] Choi WY, Kwon JM, Lee JJ, et al. Single-stage soft-switching converter with boost type of active clamp for wide input voltage ranges. IEEE Trans Power Electron. 2009;24(3):730–741.

[19] Mousavi A, Das P, Moschopoulos G. A novel ZCS-PWM full-bridge converter with a simple active auxiliary circuit. 2012 Twenty-seventh Annual IEEE Applied Power Electronics Conference and Exposition (APEC); Orlando, FL; 2012, p. 1273–1277.

[20] Averberg A, Meyer KR, Mertens A. Design considerations of a current-fed DC–DC converter with high voltage gain for fuel cell applications. 2009 13th European Conference on Power Electronics and applications; Barcelona; 2009, p. 1–10.

[21] Kim HJ, Leu CS, Farrington R, et al. Clamp mode zero-voltage-switched multi-resonant converters. Power Electronics Specialists Conference, 1992. PESC '92 Record., 23rd Annual IEEE, Toledo; 1992.

[22] Tanaka H, Ninomiya T, Shoyama M, et al. Steady-state analysis of a ZVS-PWM series resonant converter with active-clamp technique. PESC 98 Record. 29th Annual IEEE power Electronics Specialists Conference (Cat. No.98CH36196), Fukuoka; 1998, p. 655–661, Vol.1.

[23] Garcia FS, Pomilio JA, Spiazzi G. Comparison of non-insulated, high-gain, high-power, step-up DC–DC converters. 2012 Twenty-seventh Annual IEEE Applied Power Electronics Conference and Exposition (APEC); Orlando, FL; 2012, p. 1343–1347 .

[24] Park S, Choi S. Soft-switched CCM boost converters with high voltage gain for high-power applications. IEEE Trans Power Electron. 2010;25(5):1211–1217.

[25] Kwon M, Oh S, Choi S. High gain soft-switching bidirectional DC–DC converter for eco-friendly vehicles. IEEE Trans Power Electron. 2014;29(4):1659–1666.

[26] Patii D, Rathore AK, Srinivasan D, et al. High-frequency soft-switching LCC resonant current-fed DC/DC converter with high voltage gain for DC microgrid application. IECON 2014 – 40th Annual Conference of the IEEE Industrial Electronics Society; Dallas, TX; 2014, p. 4293–4299.

[27] Rathore AK, Patil DR, Srinivasan D. Non-isolated bidirectional soft-switching current-fed LCL resonant DC/DC converter to interface energy storage in DC microgrid. IEEE Trans Ind Appl. 2016;52(2):1711–1722.

[28] Wang H, Xia M, Zhu Z, et al. High-efficiency bidirectional DC/DC converter with high-gain. 2010 Asia-Pacific Power and Energy Engineering Conference, Chengdu, 2010, p. 1–5.